Unusual magnetic excitations in the weakly ordered spin-1/2 chain antiferromagnet Sr_{2}CuO_{3}: Possible evidence for Goldstone magnon coupled with the amplitude mode

E. G. Sergeicheva, S. S. Sosin, L. A. Prozorova, G. D. Gu, and I. A. Zaliznyak

Phys. Rev. B **95**, 020411 — Published 18 January 2017

DOI: 10.1103/PhysRevB.95.020411

Unusual magnetic excitations in a weakly ordered spin-1/2 chain antiferromagnet Sr_2CuO_3: Possible evidence for Goldstone magnon coupled with the amplitude mode

E. G. Sergeicheva,[1] S. S. Sosin,[1,*] L. A. Prozorova,[1] G. D. Gu,[2] and I. A. Zaliznyak[2,†]

[1]*P. Kapitza Institute for Physical Problems, 119334, Moscow, Russia*
[2]*CMPMSD, Brookhaven National Laboratory, Upton, New York 11973, USA*

(Dated: December 6, 2016)

We report on an electron spin resonance (ESR) study of a nearly one-dimensional (1D) spin$-1/2$ chain antiferromagnet, Sr_2CuO_3, with an extremely weak magnetic ordering. The ESR spectra at $T > T_N$, in the disordered Luttinger-spin-liquid phase reveal nearly ideal Heisenberg-chain behavior with only very small, field-independent linewidth, $\sim 1/T$. In the ordered state, below T_N, we identify field-dependent antiferromagnetic resonance (AFMR) modes, which are well described by the pseudo-Goldstone magnons in the model of a collinear biaxial antiferromagnet. Additionally, we observe a major resonant mode with unusual and strongly anisotropic properties, which is not anticipated by the conventional theory of Goldstone spin waves. We propose that this unexpected magnetic excitation can be attributed to a field-independent magnon mode renormalized due to its interaction with the high-energy amplitude mode in the regime of a weak spontaneous symmetry breaking.

PACS numbers: 75.50.Ee, 76.60.-k, 75.10.Jm, 75.10.Pq

The symmetry broken states and quasi-particle excitations in condensed matter explore much of the same physics as the field theories of particles in the Universe [1–8], while presenting an advantage of being precisely tunable and accessible in laboratory-scale experiments. Studying model material systems such as quantum magnets can bring important insights into the physics of strings [1–3], quark confinement, or Higgs particles [9–11]. Weakly interacting Heisenberg spin-1/2 chains present particularly favorable opportunity for exploring these concepts [4–10, 12–15].

The ground state of an isolated chain is disordered, with the de-confined fractional spin-1/2 excitations (spinons) forming a continuum of physically accessible spin-1(2,3,...) states [4, 9, 15]. This state, known as Luttinger liquid (LL), is quantum-critical, so that even a tiny inter-chain coupling in a real material leads to a three-dimensional (3D) magnetic ordering at $T < T_N$. A spontaneous symmetry breaking by magnetic order imposes linear attractive potential, which at low energy confines pairs of spin-1/2 spinons into spin-1 magnons, in accord with the Goldstone theorem requiring such gapless excitations [16, 17]. In the case of a collinear antiferromagnetic (AFM) order, these are the well-known transverse spin waves [18, 19]. The interaction of such Goldstone magnons with the amplitude fluctuations of the order parameter is usually discarded, although it must grow in importance near the quantum critical point (QCP), where the symmetry-breaking order is weak, and its amplitude fluctuations are significant. If so, what is the energy scale where this interaction occurs, and what is the spectral weight involved – are coherent Goldstone magnons detectable at all near the QCP, when the symmetry breaking is weak? What is the role of the longitudinal magnon mode predicted by the chain-mean-field (CMF) theory [12–14, 20, 21]?

Motivated by these questions, we carried out ESR experiments aimed at a comparative study of magnetic resonance in the ordered and LL phases of a chain cuprate, Sr_2CuO_3, at frequencies of the microwave field, ν, probing magnetic excitations with energies $h\nu \lesssim k_B T_N$. Surprisingly, not only we have been able to identify Goldstone magnons, modes corresponding to the transverse oscillations of the magnetic order parameter and a hallmark of spinon confinement, but we have also discovered an unusual magnetic excitation with strongly field-dependent energy gap (mass). This mode is not predicted by the low-energy, hydrodynamic theory of spin dynamics, which instead predicts a field-independent pseudo Goldstone spin wave [18, 19]. Therefore, the observed massive mode likely involves a short-wavelength physics, such as the interaction of a Goldstone magnon with the amplitude fluctuations of an order parameter [22–24].

Sr_2CuO_3 has a body-centered orthorhombic crystal structure (space group $Immm$) composed of chains of corner-sharing CuO_4 square plaquettes in the (ab)-plane, running along the b-axis of the crystal. The strong Cu-O hybridization results in an extremely strong Cu-O-Cu in-chain superexchange, $J \approx 2800$ K, [15, 25, 26]. Small orbital overlaps between the planar CuO_4 plaquettes on neighbor chains yield a much smaller inter-chain coupling, $J'/J \lesssim 5 \cdot 10^{-4}$, resulting in an almost ideal spin-chain structure. Hence, Sr_2CuO_3 undergoes a phase transition into an antiferromagnetically ordered state only below the Néel temperature $T_N = 5.5(1)\,\mathrm{K} \approx 2 \cdot 10^{-3} J$, in a very close proximity of the 1D LL quantum-critical state. Strong quantum fluctuations result in an ordered moment of only $\langle\mu\rangle = 0.06\mu_\mathrm{B}$, as was determined from neutron scattering and μSR experiments [27]. Consequently, Sr_2CuO_3 presents an ideal model material for exploring effects of an extremely weak symmetry breaking in a system of coupled quantum-critical spin-1/2 chains with fractional spinon excitations, the emergence of Goldstone and amplitude fluctuations modes resulting from spinon confinement, and the corresponding dimensional cross-over regimes.

The ESR experiments were carried out on a high-quality single crystal sample ($m \approx 0.056$ g), similar to the ones used in our previous studies [15]. The sample was oriented using the tabletop Laue Xray. The magnetic resonance spectra were

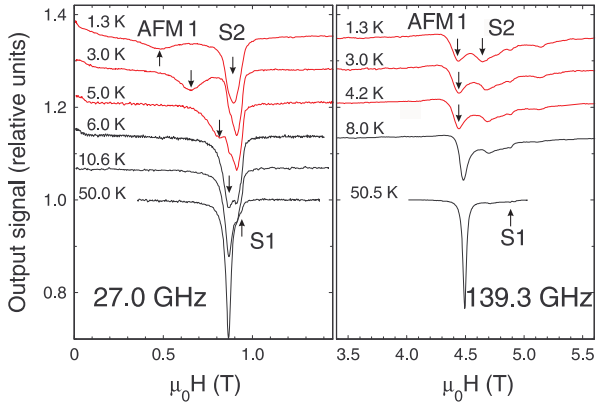

FIG. 1. Temperature dependence of magnetic resonance spectra measured at $\nu = 27.0$ GHz (left panel) and $\nu = 139.3$ GHz (right panel) for magnetic field $H \parallel c$-axis of the sample. The signals are normalized to a unit level at maximum and consecutively shifted by +0.07, from bottom to top. Red and black curves correspond to ordered and spin-liquid phases, respectively. Arrows mark different resonance peaks discussed in the text.

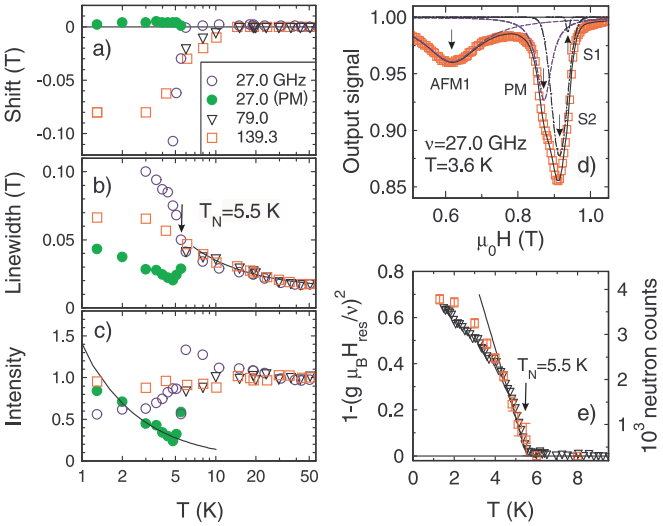

FIG. 2. The resonance field shift (a), the line width (HWHM) (b), and the integral intensity (c) of the principal ESR line as a function of temperature, measured at three excitation frequencies: 27.0 GHz (○ and ● are the two spectral components below T_N), 79.0 GHz (△), and 139.3 GHz (□), for $H \parallel c$. Solid lines in panels (b), (c) show $\alpha+\beta/T$ and C/T fits, respectively, for the width of the main line and the intensity of the residual paramagnetic component associated with defects. (d) The decomposition of a typical low-frequency resonance line in the ordered phase into Lorentzian (AFM1, PM) and Gaussian (S1, S2) spectral components. (e) The square of the AFMR gap, $\Delta_1^2(T)/\nu^2$, obtained from the temperature dependence of the AFM1 resonance field measured at $\nu = 27.0$ GHz (□) and the intensity of the $(0, 0.5, 0.5)$ neutron magnetic Bragg peak (▽) vs temperature.

measured using a set of home made transmission-type microwave spectrometers with cylindrical and rectangular cavities covering the frequency range $22 - 140$ GHz. A magnetic field up to 12 T was supplied by the superconducting magnet. The temperature varied from 0.5 K (with the ^{3}He cryostat insert) to 50 K. For the complementary neutron measurements, a larger piece of a similar Sr_2CuO_3 crystal was placed in a ^{4}He flow cryostat on SPINS spectrometer at NIST Center for Neutron Research; the fixed scattered neutron energy of 3.7 meV, BeO filter after sample, and beam collimations $37' - 80' - 80' - 240'$ from sample to detector were used.

Typical resonance absorption spectra of Sr_2CuO_3 recorded at low and high frequencies are presented in Fig. 1. At $T > T_N$, the spectrum consists of an intense principal line and two weak satellites (marked S1 and S2). An excellent fit to the field profile of the ESR absorption signal for all measurement frequencies is obtained by using Lorentzian profile for the principal line and Gaussians for the satellites, resulting in three fitting parameters for each resonance line: the signal amplitude, A, the resonance field, H_{res}, and the half width at half maximum (HWHM) linewidth, ΔH. At $T > T_N$ all observed resonance modes have linear frequency-field dependence typical of a paramagnet, $h\nu = g\mu_B H_{res}$ (h is the Planck constant, μ_B is the Bohr magneton), with the g-factor values depending on the direction of the applied field. For the main line, the g-tensor components in the principal crystal axes are, $g^a = g^b = 2.03 \pm 0.02$, $g^c = 2.22 \pm 0.02$, consistent with the ab-plane geometry of the Cu $d_{x^2-y^2}$ orbital in Sr_2CuO_3 [15]. For the satellite peak S1, $g_1^a = g_1^b = 2.22 \pm 0.02$, $g_1^c = 2.03 \pm 0.02$, while the S2 mode has isotropic g-factor, $g_2 = 2.11 \pm 0.02$. As explained in detail in [28], these resonance lines correspond to two types of paramagnetic defects whose relative concentrations can be evaluated from the corresponding integral signal intensities, normalized to the main signal: $n_1 \approx 2 \cdot 10^{-5}$, $n_2 \approx 1 \cdot 10^{-3}$, thus, establishing the exceptional quality of our single crystal samples [28–30]. Below, we therefore focus the attention on the main spin system.

The temperature evolution of the principal resonance line is shown in Figure 2, (a–c). At $T > T_N$, this mode narrows with the increasing temperature, concomitantly increasing in amplitude; its position does not change except in the vicinity of the ordering transition, at $T \lesssim 1.5T_N$. The integral intensity remains practically constant, in agreement with the low-T susceptibility of a $S = 1/2$ chain [26, 31, 32]. Within the experimental accuracy, the linewidth appears to be independent of magnetic field (the excitation frequency), Fig. 2(b). Its temperature dependence is best described as $\mu_0\Delta H \simeq 0.014 + 0.2/T$ (solid line). The $1/T$ contribution can be associated with a small anisotropy of the weak interchain coupling, $J'_z \neq J'_{x,y}$ [33], where our estimate yields $\delta J' \sim 0.5$ K, while the constant term accounts for other contributions. According to Refs. [34–36], the absence of a measurable $\sim 1/T^2$ contribution to the linewidth, as well as a very small observed $T-$dependent line shift, impose stringent upper limit on possible staggered fields, $h_{st} \lesssim 2 \cdot 10^{-2}$ K, consistent with the ideal crystal structure of Sr_2CuO_3 where such terms are prohibited by symmetry. The estimated upper bound on the $T-$linear contribution to the linewidth indicates an upper bound on the anisotropy of the intra-chain exchange, $\delta J/J \lesssim 1.4 \cdot 10^{-2}$, [28, 35], which is further corroborated by the analysis of the AFMR spectra observed below T_N. The overall detailed analysis of the high-temperature magnetic res-

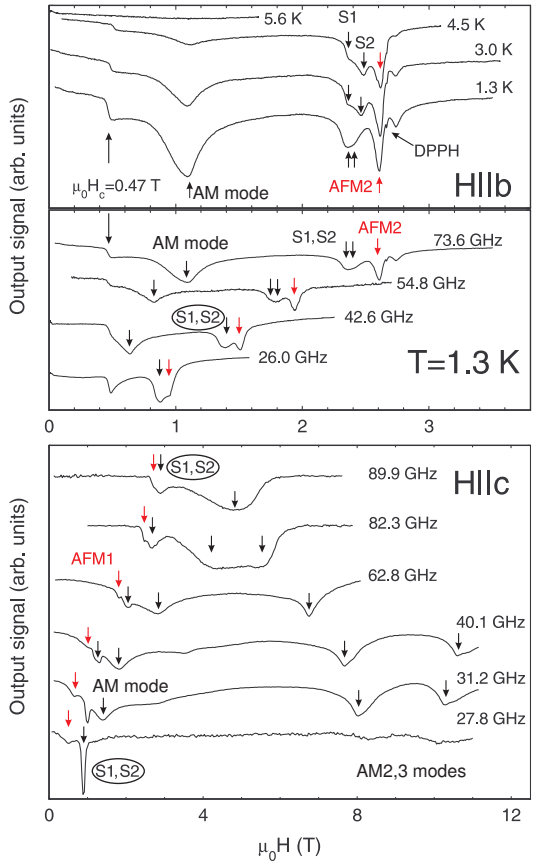

FIG. 3. The resonance absorption spectra measured for $H \parallel b$-axis at frequency $\nu = 73.6$ GHz on decreasing the temperature from above T_N to 1.3 K (upper panel), and the low-temperature records made at various excitation frequencies for $H \parallel b$ (middle panel) and $H \parallel c$ (lower panel). Arrows mark absorption maxima corresponding to different resonance modes discussed in the text.

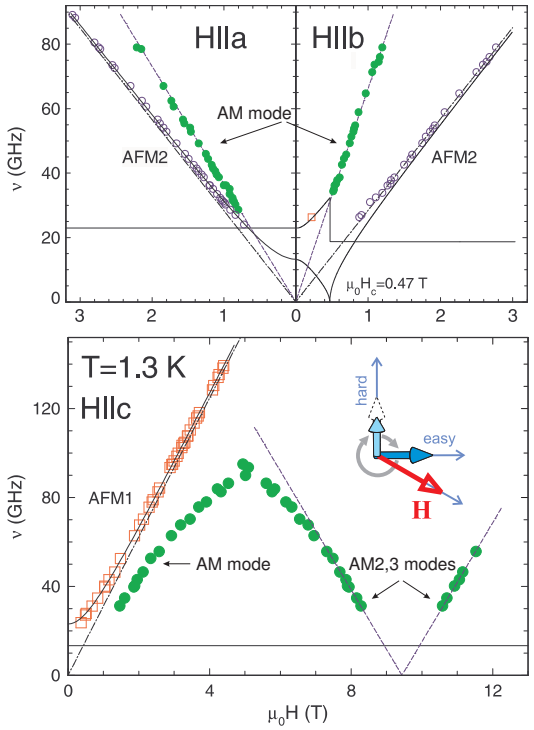

FIG. 4. Frequency-field diagrams of the magnetic resonance spectra measured at $T = 1.3$ K for the three principal directions of the applied field with respect to the crystal axes, $H \parallel a, b$ (top), and $H \parallel c$ (bottom). The two AFMR modes are shown with the open symbols, the solid lines are the theoretical calculations [18, 19, 39] for the biaxial collinear antiferromagnet. Closed circles show the low-temperature AM mode; the dashed lines are linear fits discussed in the text. The dashed-dotted lines show the paramagnetic resonance position for the g-factors obtained from high-temperature measurements. The drawing in the lower panel illustrates a mechanism of dynamical coupling of the amplitude mode and the transverse Goldstone magnon corresponding to oscillations of the order parameter in the plane perpendicular to the applied field.

onance properties of Sr_2CuO_3 is presented in Ref. [28].

At temperatures below the transition into an ordered state, the resonance spectrum of Sr_2CuO_3 markedly transforms. We observe a gradual shift of the principal resonance line, at all measurement frequencies, ν, for $H \parallel a$ and c, and in the low-frequency range for $H \parallel b$, which is consistent with the opening of gaps in the spin excitations spectrum (see upper curves in Fig. 1) [37]. Assuming the relation for a field-dependent gapped mode in a two-sublattice antiferromagnet with weak anisotropy, $\nu^2 = \Delta^2(T) + (g\mu_B/h)^2 H_{res}^2$, we obtain the temperature dependence of the gap, $\Delta(T)$, which is directly related to the AFM order parameter, $\Delta \propto \langle S \rangle$ [38]. The corresponding $(\Delta(T)/\nu)^2$ dependence for $H \parallel c$ and $\nu = 27.0$ GHz is shown in Fig. 2(e), along with the intensity of the $(0, 0.5, 0.5)$ magnetic Bragg peak measured by neutron diffraction, which also probes the square of the magnetic order parameter. The excellent agreement between the two measurements confirms unambiguously that we observe the AFMR, and that pseudo Goldstone magnon modes develop at $T < T_N$ in a system of weakly ordered chains in Sr_2CuO_3 in the frequency range probed in our experiments. The fit of the square of the order parameter in the vicinity of the ordering transition reveals linear temperature dependence consistent with the CMF theory [20], and yields the Néel temperature $T_N = 5.5(1)$ K in agreement with previous studies [27]. The evolution of satellite modes S1, S2 below T_N supports the conclusion that these signals originate from tiny amounts of defects and inclusions.

For $H \parallel b$, a step-like, non-resonant feature develops below T_N, in addition to the resonance modes (Fig. 3, upper and middle panels). The magnetic field at which this feature arises, $\mu_0 H_c \simeq 0.47$ T, does not depend on temperature and frequency. This allows its identification with a spin-flop transition [40–42], where a discontinuity in the real part of magnetic susceptibility leads to a step-like absorption feature (note that at zero field the ordered magnetic moments in Sr_2CuO_3 are directed along the b-axis [27]).

The behavior of the AFMR modes identified in our experiments for all directions of the applied magnetic field reveals the spectrum of a collinear antiferromagnet with two inequivalent anisotropy axes (in accord with the orthorhombic symmetry of Sr_2CuO_3). The most general theoretical interpretation

of the low-energy spin dynamics of such a system is provided by the theory of spin hydrodynamics [19]. For a collinear antiferromagnet, such as Sr_2CuO_3 at $T < T_N$, this phenomenological theory predicts two pseudo Goldstone transverse spin wave branches, which correspond to our AFMR modes 1 and 2. Their resonance excitation energies for all three directions of magnetic field are accurately reproduced by the theory using only two parameters, $\Delta_1 = 23.0$ GHz and $\Delta_2 = 13.3$ GHz, for the gap values rendered by a small anisotropy to the two Goldstone magnons (lines AFM1 and AFM2, respectively). The critical field of the spin-flop transition, which at low temperature is given by the relation, $\mu_0 H_c = h\Delta_2/(g^b\mu_B) \simeq 0.47$ T, is in excellent agreement with the observed value.

Having thus unambiguously established spinon confinement into the Goldstone magnons giving rise to the AFMR in Sr_2CuO_3 in the energy range covered in our measurements, $h\nu \lesssim k_B T_N$, we now focus on another remarkable feature. For all directions of the magnetic field, we observe an intense line of resonance absorption, marked "AM" (amplitude mode) in Fig. 3. It has a roughly temperature-independent line width, several times larger than that of the AFMR modes. This line appears below T_N and rapidly grows in intensity, with no shift of the resonance field, on further cooling. It reveals a novel magnetic excitation emerging in the ordered phase, which is both theoretically unanticipated and hitherto unobserved. For $H \parallel a, b$ this type of signal consists of a single resonance line; for $H \parallel b$ it only appears at $H > H_c$ (see middle panel of Fig. 3). Two additional signals are observable in the high-field range for $H \parallel c$, whose intensity drops precipitously at $\nu \lesssim 30$ GHz (see data at 27.8 GHz and 31.2 GHz in Fig. 3).

The frequency-magnetic field diagram of Fig. 4 shows the experimental data for the field dependence of this novel mode (closed symbols) along with that of the conventional AFMR lines 1, 2. For $H \parallel a, b$, the AM follows linear dependence, $h\nu = g_{eff}\mu_B H$, shown by dashed lines in the corresponding panels of Fig. 4. The fit yields a very large and anisotropic "effective $g-$factors", $g^a_{eff} = 2.60(5)$ and $g^b_{eff} = 4.7(1)$. The triple line observed for $H \parallel c$ has a non-monotone field dependence, and appears to soften in high fields, possibly indicating a quantum phase transition. In the vicinity of the "transition", $\mu_0 H_{c2} \simeq 9.44$ T, the mode can be described by a critical-type linear dependence, $h\nu = g^c_{eff}\mu_B|H - H_{c2}|$, with a slope $g^c_{eff} = 1.91(5)$ (dashed line in Fig. 4).

The nature of the spin system in Sr_2CuO_3 suggests that the new mode could be related to the amplitude fluctuations of the order parameter in a weakly ordered system of spin-1/2 AFM chains. We note that no such mode was observed in $CsNiCl_3$, a system of weakly coupled AFM spin-1 chains with a very similar $T_N \approx 4.8$ K, nor in a spin-5/2 chain system $CsMnBr_3$ ($T_N \approx 8$ K), where the ESR spectra are in full agreement with the spin hydrodynamics theory [43, 44]. In Sr_2CuO_3 the theory predicts an undetectable (for our field-scanning technique), field-independent AFMR modes (horizontal lines in Fig. 4), in addition to the observed field-dependent pseudo Larmor (lines 1 or 2, depending on the field direction). An interaction of these Goldstone magnons with the amplitude mode of the order parameter provides a plausible mechanism by which they can acquire field dependent mass. At the origin of such coupling could be the spin anisotropy, which favors different amplitude of the ordered moment depending on its alignment with respect to the easy/medium/hard axis. This is illustrated in the lower panel of Fig. 4, where the Larmor precession of the ordered magnetic moment around the applied field modulates its amplitude.

In summary, our ESR measurements in the quasi-1D spin-1/2 chain antiferromagnet Sr_2CuO_3 confirm nearly ideal 1D Heisenberg behavior in the Luttinger-liquid phase. In the weakly ordered AFM phase, at $T < T_N$, they reveal a novel, dominant excitation mode, which develops along with the field-dependent gapped AFMR modes (transverse pseudo-Goldstone magnons) intrinsic to a collinear antiferromagnet with weak two-axial anisotropy. Recent analysis [45] of the Heisenberg necklace model performed in the context of the present findings suggests that such a strongly field-dependent excitation cannot be explained by a coupling to the paramagnetic impurities, or the nuclear spins, and therefore must be a property of the bulk chains. This new mode is missed by the macroscopic theory of spin hydrodynamics, which provides theoretical interpretation for the pseudo Goldstone spin waves observed in our experiments. It thus embodies a short-wavelength physics and can be rationalized as a mixed mode of the transverse and the amplitude fluctuations of the order parameter [22–24], resulting from the interaction of the Goldstone magnon with the Higgs amplitude mode (AM) [46]. Consistent with this mixed character is its substantial width, reflecting the universally damped amplitude mode, and broad longitudinal modes found in other experiments [12–14]. The observed softening of the novel AM mode at a critical field H_{c2} might then herald a symmetry breaking transition to the longitudinal spin density wave state, which is expected in a system of weakly coupled spin-1/2 chains in a field [47].

The authors thank A. I. Smirnov, L. E. Svistov, V. N. Glazkov, M. E. Zhitomirsky, A. Abanov and A. Tsvelik for useful discussions. The work at P. Kapitza Institute was supported by the Russian Fund for Basic Research, Grant 15-02-05918, and the Program of Russian Scientific Schools. The work at Brookhaven National Laboratory was supported by the Office of Basic Energy Sciences, U.S. Department of Energy, under Contract No. DE-SC00112704. We acknowledge the support of NIST, US Department of Commerce, in providing the neutron research facilities used in this work.

* sosin@kapitza.ras.ru
† zaliznyak@bnl.gov

[1] A. Polyakov, Nuclear Physics B **120**, 429 (1977).
[2] J. B. Kogut, Rev. Mod. Phys. **51**, 659 (1979).
[3] D. M. Hofman and J. M. Maldacena, Journal of High Energy Physics **2007**, 063 (2007).
[4] F. Haldane, Physics Letters A **93**, 464 (1983).

[5] A. M. Tsvelik, *Quantum Field Theory in Condensed Matter Physics*, 2nd ed. (Cambridge University Press, 2003).

[6] E. Fradkin, *Field Theories of Condensed Matter Physics* (Cambridge University Press, 2013).

[7] N. Nagaosa and S. Heusler, *Quantum Field Theory in Strongly Correlated Electronic Systems*, Theoretical and Mathematical Physics (Springer Berlin Heidelberg, 1999).

[8] G. Grignani and G. W. Semenoff, "Introduction to some common topics in gauge theory and spin systems," in *Field Theories for Low-Dimensional Condensed Matter Systems: Spin Systems and Strongly Correlated Electrons*, edited by G. Morandi, P. Sodano, A. Tagliacozzo, and V. Tognetti (Springer Berlin Heidelberg, Berlin, Heidelberg, 2000) pp. 171–233.

[9] B. Lake, A. M. Tsvelik, S. Notbohm, D. Alan Tennant, T. G. Perring, M. Reehuis, C. Sekar, G. Krabbes, and B. Buchner, Nat Phys **6**, 50 (2010).

[10] Z. Wang, M. Schmidt, A. K. Bera, A. T. M. N. Islam, B. Lake, A. Loidl, and J. Deisenhofer, Phys. Rev. B **91**, 140404 (2015).

[11] P. Merchant, B. Normand, K. W. Kramer, M. Boehm, D. F. McMorrow, and C. Ruegg, Nat Phys **10**, 373 (2014).

[12] B. Lake, D. A. Tennant, C. D. Frost, and S. E. Nagler, Nat Mater **4**, 329 (2005).

[13] B. Lake, D. A. Tennant, and S. E. Nagler, Phys. Rev. B **71**, 134412 (2005).

[14] A. Zheludev, K. Kakurai, T. Masuda, K. Uchinokura, and K. Nakajima, Phys. Rev. Lett. **89**, 197205 (2002).

[15] A. C. Walters, T. G. Perring, J.-S. Caux, A. T. Savici, G. D. Gu, C.-C. Lee, W. Ku, and I. A. Zaliznyak, Nat Phys **5**, 867 (2009).

[16] I. A. Zaliznyak, Nat Mater **4**, 273 (2005).

[17] J. Goldstone, A. Salam, and S. Weinberg, Phys. Rev. **127**, 965 (1962).

[18] A. F. Andreev, Zh. Éksp. Teor. Fiz. **74** (1978); Soviet Journal of Experimental and Theoretical Physics **47**, 411 (1978).

[19] A. F. Andreev and V. I. Marchenko, Usp. Fiz. Nauk **130**, 39 (1980); Soviet Physics Uspekhi **23**, 21 (1980).

[20] H. J. Schulz, Phys. Rev. Lett. **77**, 2790 (1996).

[21] F. H. L. Essler, A. M. Tsvelik, and G. Delfino, Phys. Rev. B **56**, 11001 (1997).

[22] P. W. Higgs, Rev. Mod. Phys. **86**, 851 (2014).

[23] G. E. Volovik and M. A. Zubkov, Journal of Low Temperature Physics **175**, 486 (2013).

[24] D. Pekker and C. Varma, Annual Review of Condensed Matter Physics **6**, 269 (2015).

[25] H. Suzuura, H. Yasuhara, A. Furusaki, N. Nagaosa, and Y. Tokura, Phys. Rev. Lett. **76**, 2579 (1996).

[26] N. Motoyama, H. Eisaki, and S. Uchida, Phys. Rev. Lett. **76**, 3212 (1996).

[27] K. M. Kojima, Y. Fudamoto, M. Larkin, G. M. Luke, J. Merrin, B. Nachumi, Y. J. Uemura, N. Motoyama, H. Eisaki, S. Uchida, K. Yamada, Y. Endoh, S. Hosoya, B. J. Sternlieb, and G. Shirane, Phys. Rev. Lett. **78**, 1787 (1997).

[28] See supplementary information for additional discussion.

[29] K. M. Kojima, J. Yamanobe, H. Eisaki, S. Uchida, Y. Fudamoto, I. M. Gat, M. I. Larkin, A. Savici, Y. J. Uemura, P. P. Kyriakou, M. T. Rovers, and G. M. Luke, Phys. Rev. B **70**, 094402 (2004).

[30] J. Sirker, N. Laflorencie, S. Fujimoto, S. Eggert, and I. Affleck, Phys. Rev. Lett. **98**, 137205 (2007).

[31] S. Eggert, I. Affleck, and M. Takahashi, Phys. Rev. Lett. **73**, 332 (1994).

[32] O. A. Starykh, R. R. P. Singh, and A. W. Sandvik, Phys. Rev. Lett. **78**, 539 (1997).

[33] S. C. Furuya and M. Sato, Journal of the Physical Society of Japan **84**, 033704 (2015).

[34] M. Oshikawa and I. Affleck, Phys. Rev. Lett. **82**, 5136 (1999).

[35] M. Oshikawa and I. Affleck, Phys. Rev. B **65**, 134410 (2002).

[36] Y. Maeda, K. Sakai, and M. Oshikawa, Phys. Rev. Lett. **95**, 037602 (2005).

[37] For $H \parallel c$, in addition to the gapped AFMR mode that develops below T_N, a residual signal at the original paramagnetic position of the principal resonance line is observed at low frequencies. The decomposition of the typical resonance spectrum recorded at $\nu = 27.0$ GHz and $T = 3.6$ K into four components is shown in Fig. 2(d). On cooling below T_N, the integral intensity of the "paramagnetic" component roughly follows the Curie law [closed symbols in Fig. 2(c)], which lets us associate this signal with a small amount, $n_i \lesssim 5 \cdot 10^{-4}$, of in-chain/end-of-chain defects. Their contribution is not discernable at high frequency, $\nu = 139.3$ GHz (Fig. 2), where we only observe a slight shift of the resonance line to lower fields, consistent with the opening of the gap, $\Delta(T)$. While the low-frequency resonance exhibits a pronounced anomaly at $T = T_N$, at high frequency it is less sensitive to the transition into an ordered state (Fig. 2).

[38] L. A. Prozorova and A. S. Borovik-Romanov, Zh. Éksp. Teor. Fiz **55**, 1727–1736 (1968); Soviet Journal of Experimental and Theoretical Physics **28**, 910 (1969).

[39] T. Nagamiya, K. Yosida, and R. Kubo, Advances in Physics **4**, 1 (1955).

[40] S. Foner and S.-L. Hou, Journal of Applied Physics **33** (1962).

[41] M. L. Plumer, K. Hood, and A. Caillé, Phys. Rev. Lett. **60**, 45 (1988).

[42] O. Petrenko, S. Petrov, and L. Prozorova, Zh. Éksp. Teor. Fiz. **98**, 727 (1990); Soviet Physics - JETP **71**, 406 (1990).

[43] I. A. Zaliznyak, V. I. Marchenko, S. V. Petrov, L. A. Prozorova, and A. V. Chubukov, Pis'ma Zh. Eksp. Teor. Fiz. **47**, 172 (1988); JETP Lett **47**, 211 (1988).

[44] I. Zaliznyak, L. Prozorova, and S. Petrov, Zh. Éksp. Teor. Fiz. **97**, 359 (1990); Soviet Physics - JETP **70**, 203 (1990).

[45] A. M. Tsvelik and I. A. Zaliznyak, Phys. Rev. B **94**, 075152 (2016).

[46] M. Powalski, G. S. Uhrig, and K. P. Schmidt, Phys. Rev. Lett. **115**, 207202 (2015).

[47] B. Grenier, V. Simonet, B. Canals, P. Lejay, M. Klanjšek, M. Horvatić, and C. Berthier, Phys. Rev. B **92**, 134416 (2015).